Optimising speed and frequency of a scale model smooth vibrating drum roller on lunar highland regolith simulant

Akshay K. Agarwal,[1] Brendan T. Scott, Ph.D.,[1] and Mark B. Jaksa, Ph.D.[1]

[1]School of Civil Engineering and Construction Management, Adelaide University, SA, 5005, Australia; e-mail: akshaykumar.agarwal@adelaide.edu.au

ABSTRACT

As part of NASA's Artemis program, establishing a sustainable lunar base near the Moon's South Pole is a key objective. Understanding the effects of compaction on the lunar surface is essential to support infrastructure development and long-term exploration activities. This study presents the results of laboratory experiments conducted using a scaled lunar vibrating drum roller (LVDR-1) to investigate the densification behaviour of lunar highland regolith simulant. LVDR-1 used in this study had two different roller masses: 2.92 kg and 4.45 kg. Besides mass, experiments conducted evaluated the effects of varying roller speed and motor frequency. Key metrics such as surface settlement and roller-induced vertical pressure were measured to assess compaction effectiveness. The vertical pressure results were most influenced by the frequency at which the LVDR-1 operated. For the 2.92 kg mass, the highest peak pressures were observed at 2 km/h and 40 Hz, whilst for the 4.45 kg mass, 6 km/h and 40 Hz were found to be optimal, confirming that the optimal combination of speed and frequency differs with roller mass.

KEYWORDS: lunar construction, vibrating smooth drum roller, mass, frequency, speed.

1. INTRODUCTION

The National Aeronautics and Space Administration (NASA) seeks to establish the Moon as a strategic hub for sustained deep space exploration. A central objective of this initiative is the construction of a lunar base in the highland region near the Moon's South Pole. However, the lunar surface is covered by an unconsolidated layer of fine debris, known as regolith (Carrier III et al., 1991), which presents significant engineering challenges.

Translating terrestrial construction practices to the lunar environment requires a comprehensive understanding of the Moon's unique geotechnical and environmental conditions. Compared to Earth, the Moon has a gravitational acceleration approximately one-sixth that of Earth's, lacks both water and atmospheric pressure, and experiences extreme temperature fluctuations that occur between lunar day and night (Vaniman et al., 1991). These conditions significantly influence soil behaviour and consequently construction methodologies. Lunar infrastructure will require the development of roads, landing pads and structural foundations that can support heavy loads transported from landing zones to operational bases. The regolith thickness varies across the surface, ranging from 3 to 5 metres in the lunar maria region to 10 to 20 metres in the highlands region (Oravec 2009). A clear

understanding of lunar regolith compaction behaviour is, therefore, essential for designing stable and durable foundations that meet lunar mission requirements.

Agarwal et al. (2024) conducted scaled laboratory tests using the LVDR-1 vibrating smooth drum roller (VSDR) with a mass of 2.92 kg to assess its effectiveness in compacting lunar highland regolith simulant. In a subsequent study, Agarwal et al. (2025, under review) extended this work by comparing the performance of the LVDR-1 with a four-sided scale model impact roller. This work demonstrated that vibration was a more effective ground improvement technique than impact for compacting the lunar highland simulant tested.

The present study goes beyond conventional parametric variation by revealing previously unexplored dynamic interactions among mass, speed and vibration frequency for compaction of lunar highland regolith simulant. Rather than treating these parameters independently, this work identifies the interdependent relationship between these parameters that governs densification efficiency. A comprehensive experimental framework is developed to capture non-linear compaction behaviour by a vibrating smooth drum roller, which has not been reported in prior studies. The findings establish new mechanistic insights that directly inform the optimisation of lunar surface compaction systems.

This study advances the design of lunar regolith compaction strategies for in situ resource utilisation (ISRU), thereby contributing scientific understanding and engineering relevance to sustainable lunar infrastructure development.

2. BACKGROUND

In terrestrial soil compaction, air voids are typically reduced via a mechanical process involving static, dynamic, impact or vibratory loading. Agarwal et al. (2024) evaluated compaction methods suitable for lunar applications by comparing six different compaction techniques that are widely used within the terrestrial construction industry. The review identified impact rollers and vibrating smooth drum rollers (VSDRs) as the most promising techniques for lunar application. Building upon this study, Agarwal et al. (2025, under review) conducted a comparative analysis between scale models of a 4-sided impact roller and a VSDR. The experiments demonstrated that the VSDR achieved greater surface settlement, higher peak pressures across multiple depth intervals, larger densities, and a greater depth of influence than the impact roller.

The compaction performance of VSDRs has been widely studied in terrestrial applications; however, investigations specific to extraterrestrial environments, such as the lunar surface, remain limited. Wersäll (2016) highlighted the significance of vibration frequency in influencing soil compaction outcomes. In the context of lunar infrastructure development, a thorough understanding of the behaviour of lunar highland regolith simulant under varying vibratory loading conditions is essential.

In terrestrial applications, the selection of roller mass is a critical factor that directly influences the depth, uniformity and effectiveness of soil compaction. VSDRs are typically available in a range of operating masses, varying from 7,000 kg to over 20,000 kg, depending on the model and ballast configuration (Caterpillar, 2025). These varying masses are specifically designed to suit different soil types and compaction requirements in the field. To

investigate how mass affects the compaction behaviour of lunar highland regolith simulant, two distinct masses are tested: 2.92 kg and 4.45 kg.

In the present study, as well as in recent investigations by Scott et al. (2023), Agarwal et al. (2024, 2025(under review)), the same lunar highland regolith simulant has been employed. Owing to the limited availability of actual lunar highland regolith samples, simulants are routinely adopted for experimental research (Toklu & Akpinar, 2022). This study utilises LHS-1E (engineering-grade lunar highland simulant), commercially produced by Space Resource Technologies (Space Resource Technologies, 2021), previously known as Exolith Lab. LHS-1E is composed of 75% anorthosite and 25% basalt, designed to closely replicate the mineralogical composition of the actual lunar highlands regolith. Previous work by Agarwal et al. (2023) established that the geotechnical characteristics of LHS-1E are a credible surrogate for actual lunar highland regolith, particularly in the context of geotechnical and construction-related studies.

This study presents a comprehensive parametric investigation of scaled VSDRs, focusing on the compaction performance of a lunar highland regolith simulant. The current study integrates a systematic analysis of roller mass, speed and motor frequency to identify optimal combinations for efficient compaction. This investigation used surface settlement measurements and real-time monitoring using buried earth pressure cells, enabling a detailed assessment of compaction behaviour. These results establish a performance baseline while providing novel insights into operational parameters and roller mechanics, with direct implications for lunar and planetary surface construction applications.

3. METHODOLOGY

Two bins (Bin A and Bin B), each measuring 750 mm in width, 1060 mm in length, and 380 mm in depth, were used to contain the lunar highland regolith simulant, as shown in Figure 1. The lunar vibrating smooth drum roller (LVDR-1) model (Figure 2) is mobilised along the test lane via a chain-driven carriage system, powered by a variable-speed electric motor.

Figure 1. Test facility setup after lunar highland regolith simulant placement.

To investigate the compaction response of the simulant with depth under terrestrial laboratory conditions, a series of translational speed tests were undertaken. Seven distinct operating speeds in 2 km/h increments, ranging from 2 to 14 km/h, were adopted. At each speed, three motor frequencies of 20, 30, and 40 Hz were applied, resulting in 21 unique combinations of speed and drum vibration frequency.

A minimum speed of 2 km/h was selected based on the findings of Henrich (1987), who identified the optimal compaction speed range for vibratory rollers was between 1 to 4 km/h. A maximum speed of 14 km/h was chosen as it is a multiple of the speed increment and it is close to the maximum speed of Astrolab's FLEX (Flexible Logistics and Exploration) rover, a lunar surface mobility platform capable of reaching speeds of up to 15 km/h (Patrascu, 2022).

An externally mounted electric motor fitted with an eccentric mass was integrated into the scale model to control vibrational frequency. The rotating eccentric mass generates periodic inertial forces, resulting in dynamic loading that can be precisely regulated through adjustment of the motor speed. This configuration allows for repeatable and consistent frequency conditions during testing. With regard to vibration frequency, three discrete values of 20, 30, and 40 Hz were selected to span the range of the vibratory motor, which was limited due to mechanical constraints. Although Henrich (1987) recommends a frequency range of 25–45 Hz, the three chosen values provided sufficient resolution to examine the influence of vibration on the lunar simulant while remaining within the limits of the equipment. It is also important to acknowledge that the compaction behaviour of actual lunar regolith may vary under the Moon's unique environmental conditions, which include low gravity, vacuum exposure, and the presence of electrostatically charged particles.

As mentioned, these tests were conducted using two different roller masses: 2.92 kg and 4.45 kg, producing a total of 42 test combinations. Figure 2 presents the scale model of the VSDR utilised in the compaction experiments carried out on the test lane. The initial configuration featured a drum mass of 2.92 kg (Figure 2a), and an additional mass was subsequently affixed to the top of the model to increase the mass by approximately 50%, resulting in a total drum mass of 4.45 kg (Figure 2b). In this configuration, four rectangular blocks were mounted by screws on the sides of the motor—two on each side—within the frame, without contacting the drum. It should be noted that this represents a limitation of the scale model design, as increasing the mass is only possible by placing additional mass on top of the drum in lieu of placing eccentric masses inside the drum roller. The scale model incorporates a drum of width 165 mm and a diameter of 100 mm, closely representing the scaled dimensions of full-sized terrestrial rollers. Vibration is generated via an eccentrically-loaded electric motor mounted on the drum axle (Figure 2c), effectively emulating the vibratory mechanism found in conventional field compaction equipment. To confirm the operational frequency of the motor, a Fast Fourier Transform (FFT) analysis was performed on earth pressure cells data (discussed below) for each of the 42 test combinations. This analysis verified the actual frequency applied in each combination.

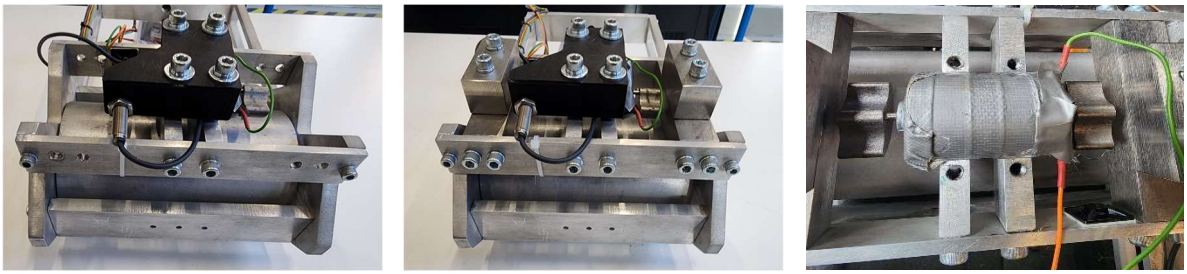

(a) (b) (c)

Figure 2. LVDR-1 scale model: (a) 2.92 kg version; (b) 4.45 kg version; (c) Electric vibration motor.

The adopted mini earth pressure cells (EPCs), as shown in Figure 3, have a diameter of 19 mm and are equipped with integrated tri-axis accelerometers. Conventional EPCs with larger diameters have been widely used in geotechnical engineering for in situ earth pressure measurements (e.g., Rinehart & Mooney 2009; Scott et al. 2019). A 3-axis accelerometer was fixed to each EPC to provide real-time information regarding the compaction of the lunar highland regolith simulant. All EPCs and accelerometers were connected to a custom-built data acquisition system, integrated with a bespoke LabVIEW interface. To accurately capture peak pressures and ground accelerations during compaction, a sampling frequency of 7,500 Hz was employed.

(a) (b)

Figure 3. Earth pressure cell: (a) Plan view; (b) Internal 3-axis accelerometers.

Error! Reference source not found. illustrates the rolling direction of and placement of EPCs within Bin B. The EPCs were installed at 100 mm intervals to ensure uniform data acquisition across the test section. As shown in **Error! Reference source not found.**a, the LVDR-1 unit traversed the designated test lane, which is located in the centre of the bin to minimise boundary effects, with the distance from the edge of the bin to the centreline of the roller lane being maintained at 375 mm. In order to achieve a homogenous target density in each bin, the simulant was weighed and carefully placed into each bin using 10-litre buckets, and pluviated through a 2.36 mm sieve, so that the simulant fell from a height no greater than 200 mm. To achieve the most uniform placement density possible, care was taken in placing the simulant in layers not exceeding 50 mm in thickness. During the placement of six EPCs within Bin B, the EPCs sensors were embedded in the lunar highland regolith simulant at a lateral spacing of 100 mm and vertical intervals of 50 mm, as illustrated in Figure 4b. Two EPCs were installed at each depth of 50, 100 and 150 mm, and the average readings from each pair were used to represent the peak pressure at that corresponding depth. All pressure cells were zeroed to account for the effects of overburden pressure such that only roller-induced pressures are reported. This configuration was designed to mitigate the influence of sensor

shadowing (Dave & Dasaka, 2011) beneath the centreline of the roller module operating in the test lane.

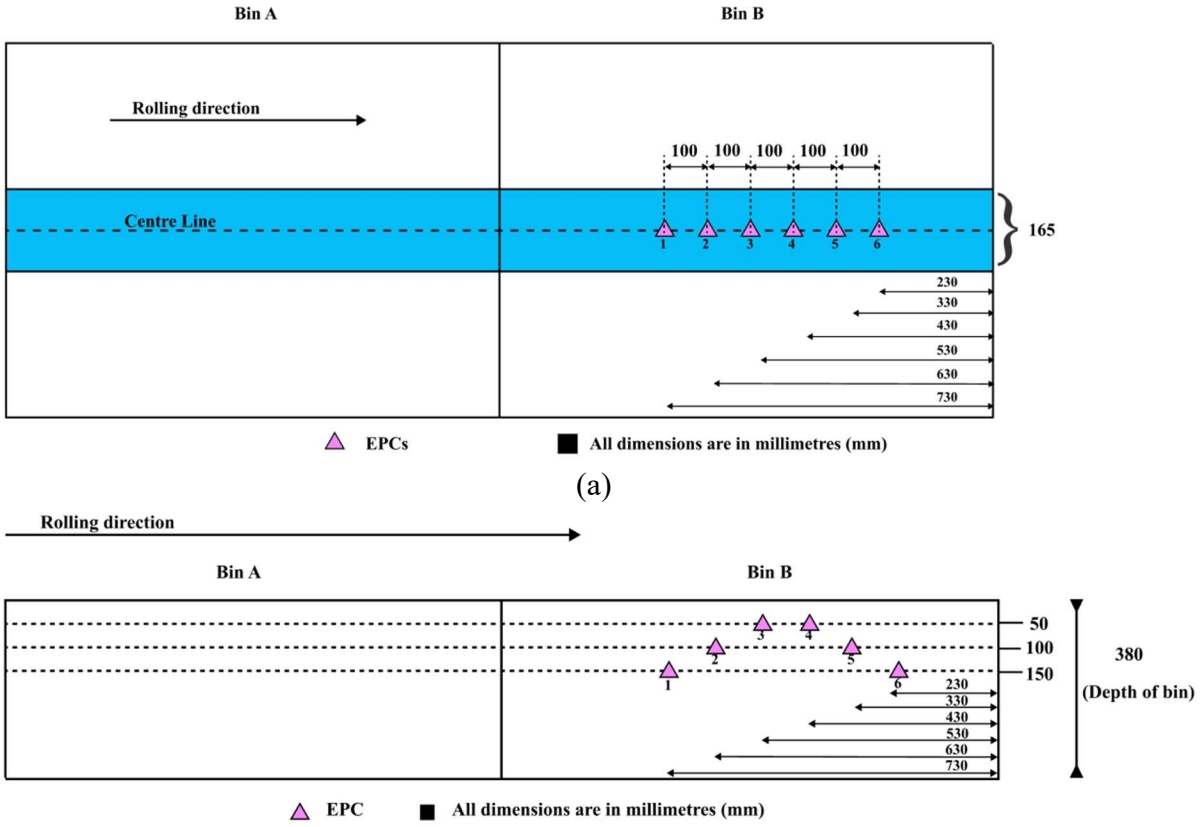

Figure 4. Placement of the EPCs: (a) Plan view; (b) Elevation view showing embedment depths.

Prior to testing the speed-frequency combinations, an initial 60 passes of the vibrating smooth drum roller were carried out at a baseline speed of 4 km/h and a vibration frequency of 30 Hz to induce the majority of surface settlement. Following this, each of the 21 unique combinations of operating speed and vibration frequency were tested. For each combination, the vibrating smooth drum roller executed 10 passes over the test lane. This procedure was repeated for both roller masses 2.92 kg and 4.45 kg, resulting in a total of 42 distinct test combinations as outlined in Table 1. The sequence of vibration frequency during testing was systematically varied to assess the influence across a full range of roller speeds. The initial vibration frequency was set to 30 Hz, at which all seven speeds were tested. After the completion of all speeds (i.e., after the 130th pass), the frequency was increased to 40 Hz, and the same speed sequence repeated. Subsequently, after the 200th pass, the frequency was reduced to 20 Hz, completing all frequency and speed testing at this roller mass.

Following the 270th pass, the roller mass was increased to 4.45 kg. A similar testing pattern was adopted: the vibration frequency was initially maintained at 30 Hz from passes 270 to 340, then increased to 40 Hz until the 410th pass, and finally reduced to 20 Hz for the remaining passes as summarised in Table 1.

The different speeds at which the model traversed the bins, measured in mm/s, were converted to their full-scale equivalents in km/h by using appropriate scaling laws and principles (Altaee & Fellenius, 1994), as presented in Table 1. Further details regarding the scale model test rig used in this study are provided by Chung et al. (2017).

Table 1. Compaction parameters at varying speeds and vibration frequencies.

Combination	Roller mass (kg)	Speed (km/h)	Speed (mm/sec)	Vibrating frequency (Hz)	Passes
0	2.92 kg	4	85	30	0-60
1		4	85	30	61-70
2		6	128	30	71-80
3		8	171	30	81-90
4		10	214	30	91-100
5		12	256	30	101-110
6		14	299	30	111-120
7		2	43	30	121-130
8		4	85	40	131-140
9		6	128	40	141-150
10		8	171	40	151-160
11		10	214	40	161-170
12		12	256	40	171-180
13		14	299	40	181-190
14		2	43	40	191-200
15		2	43	20	201-210
16		4	85	20	211-220
17		6	128	20	221-230
18		8	171	20	231-240
19		10	214	20	241-250
20		12	256	20	251-260
21		14	299	20	261-270
22	4.45 kg	4	85	30	271-280
23		6	128	30	281-290
24		8	171	30	291-300
25		10	214	30	301-310
26		12	256	30	311-320
27		14	299	30	321-330
28		2	43	30	331-340
29		4	85	40	341-350
30		6	128	40	351-360
31		8	171	40	361-370
32		10	214	40	371-380
33		12	256	40	381-390
34		14	299	40	391-400
35		2	43	40	401-410
36		2	43	20	411-420
37		4	85	20	421-430
38		6	128	20	431-440
39		8	171	20	441-450
40		10	214	20	451-460
41		12	256	20	461-470
42		14	299	20	471-480

Surface settlements were measured along the centre of the test lane. A standard tape measure was used at 150 mm intervals along the test rig track. The test rig provided a stable and repeatable datum for consistent measurements throughout the experiment. As mentioned above, for each unique combination of roller speed and vibration frequency, a total of 10 passes were performed, after which six settlement readings were recorded, and the mean value calculated to represent the surface settlement corresponding to that test combination. The initial measurements, corresponding to zero passes, were considered the baseline for assessing the impact of subsequent compaction passes.

4. RESULTS

Figure 5. Surface settlement versus number of passes. presents the surface settlement results as a function of the number of compaction passes using the VSDR on the centre lane. As expected, the most significant settlement was recorded during the initial passes, consistent with previous findings (Agarwal et al., 2024, 2025(under review)), which attributed early-stage deformation to the loose packing of the initially placed simulant.

A surface settlement of approximately 21 mm was observed within the first 35 passes, after which the rate of settlement substantially declined, indicating the onset of compaction stabilisation. As mentioned above, 60 passes were conducted at a fixed speed of 4 km/h and a vibration frequency of 30 Hz. Beyond this point, different combinations of speed and frequency were implemented to further examine the compaction behaviour. Between the 60^{th} and 130^{th} passes, VSDR operation at 30 Hz with varying roller speeds produced negligible settlement.

A notable increase in surface settlement was observed at the 140th pass, with an additional 5 mm recorded relative to the measurement at the 130th pass. This behaviour coincided with an increase in motor frequency from 30 Hz to 40 Hz, suggesting a potential correlation between higher excitation frequency and enhanced surface deformation at this stage of compaction. Between the 140th and 190th passes, only minor variations in settlement were observed under 40 Hz excitation as the roller speed was varied. However, between the 190th and 200th passes, operating the roller at a reduced speed of 2 km/h under a motor frequency of 40 Hz resulted in a marked increase in surface settlement, underscoring the influence of reduced speed on compaction effectiveness. These findings indicate that lower operational speeds, when combined with higher motor frequencies, enabling more energy to be transferred into the regolith simulant.

Following this, the motor frequency was reduced to 20 Hz, and compaction continued at varying roller speeds up to the 270th pass. During this period, no further surface settlement was observed, indicating that a lower motor frequency had negligible influence on surface deformation at this stage. This suggests that 20 Hz was insufficient to induce additional compaction, potentially due to reduced energy input and diminished dynamic interaction with the lunar highland regolith simulant.

Again, as mentioned above, following the completion of the 270th pass, the roller mass was increased from its initial configuration of 2.92 kg to 4.45 kg. The same 21 unique combinations of roller speed and motor frequency were subsequently applied using the heavier drum to further assess the effects of increased mass. It can be observed from Figure 5. Surface settlement versus number of passes. that the majority of surface deformation occurred during

the initial passes, with a clear plateauing trend observed in the later stages. This is corroborated by the measured surface settlements at the 270th and 480th passes, which were approximately 34 mm and 36 mm, respectively. As the number of passes increased, the material exhibited greater stiffness, resulting in a progressive reduction in the incremental settlement generated with each subsequent pass. These results confirm the diminishing marginal effect of additional passes on surface settlement and highlight the enhanced compaction efficiency of LVDR-1, particularly under conditions of lower roller speed and higher motor frequency. Overall, the data indicate that reduced operational speed combined with elevated motor frequency significantly improves compaction performance on lunar highland regolith simulant.

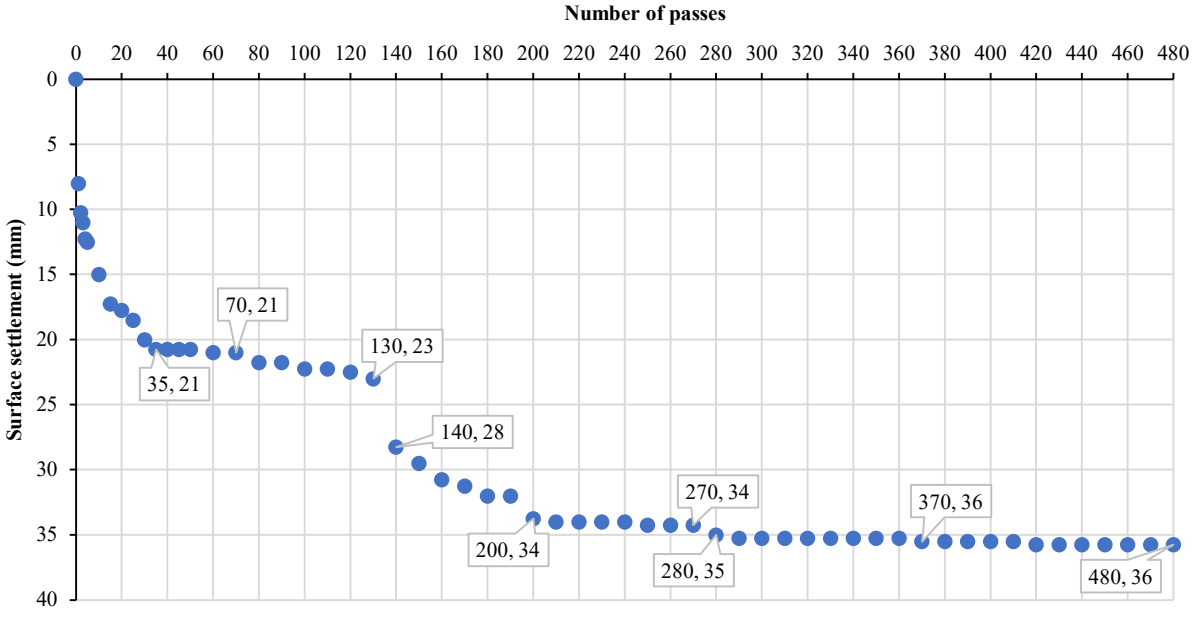

Figure 5. Surface settlement versus number of passes.

Figure 6. Peak pressure with depth for different operating speeds of LVDR-1 under motor frequencies of 20, 30, and 40 Hz, using a 2.92 kg drum roller: (a) 2 km/h, (b) 4 km/h, (c) 6 km/h, (d) 8 km/h, (e) 10 km/h, (f) 12 km/h, and (g) 14 km/h. presents the measured peak pressures plotted against depth below the ground surface using a drum roller of 2.92 kg mass for different operating speeds. For each test combination, the peak pressure readings from all six EPCs were averaged over ten roller passes at each depth. Figures 6a – 6g compare the results obtained from LVDR-1 at three motor frequencies i.e., 20 Hz, 30 Hz, and 40 Hz applied to the simulant at operating speeds of 2, 4, 6, 8, 10, 12, and 14 km/h, respectively. In this analysis, the speed is kept constant within each plot.

It can be observed that, at every speed, the 40 Hz frequency consistently produces the highest roller-induced pressure with depth. For example, in the case of the 2 km/h speed (Figure 6a), the 40 Hz curve exhibits a clear peak pressure higher than those of 20 Hz and 30 Hz. This trend remains consistent across all speeds, indicating that an increase in motor frequency of LVDR-1 leads to higher peak pressure irrespective of the operating speed.

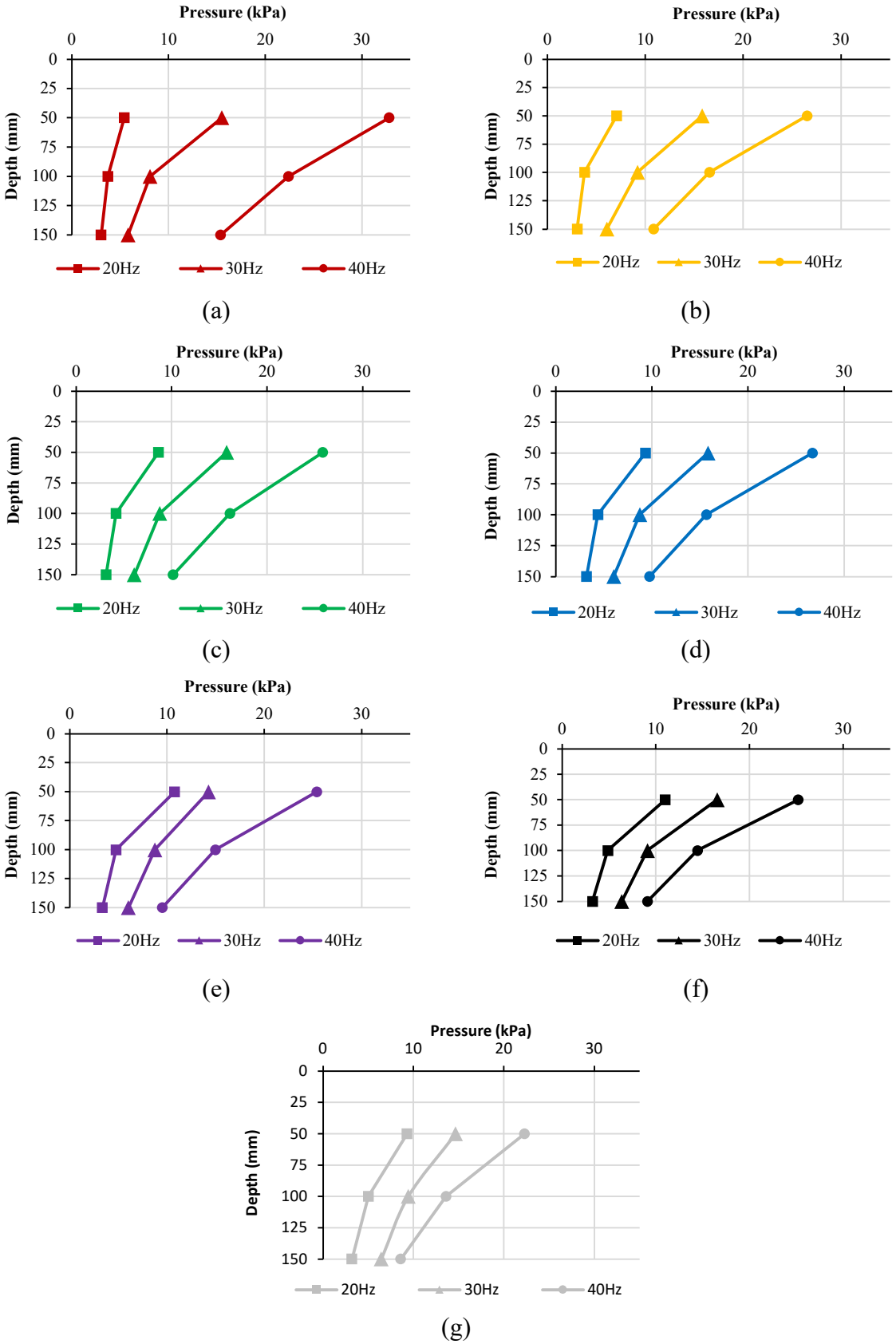

292 **Figure 6. Peak pressure with depth for different operating speeds of LVDR-1 under**
293 **motor frequencies of 20, 30, and 40 Hz, using a 2.92 kg drum roller: (a) 2 km/h, (b) 4**
294 **km/h, (c) 6 km/h, (d) 8 km/h, (e) 10 km/h, (f) 12 km/h, and (g) 14 km/h.**

Figure 7. Peak pressure with depth for different operating speeds of LVDR-1 using a 2.92 kg drum roller, at fixed motor frequencies: (a) 20 Hz, (b) 30 Hz, and (c) 40 Hz. illustrates the measured peak pressures plotted against depth when the motor frequency is kept constant and the operating speed is varied across 2, 4, 6, 8, 10, 12, and 14 km/h using a drum roller of 2.92 kg mass. Figures 7a, 7b, and 7c represent the pressure–depth response of the simulant corresponding to a constant motor frequency of LVDR-1, i.e., 20 Hz, 30 Hz, and 40 Hz, respectively. In this analysis, the motor frequency is held constant within each figure, enabling a direct evaluation of the influence of the LVDR-1 operating speed on the pressure–depth response. It is clearly observed from Figures 7a and 7b that, for motor frequencies of 20 Hz and 30 Hz, the highest peak pressures occur at an operating speed of 12 km/h, with average values of 11 kPa and 17 kPa, respectively, at a depth of 50 mm. However, at the higher motor frequency of 40 Hz, as shown in Figure 7c, the maximum peak pressure of 33 kPa was recorded at the lowest operating speed of 2 km/h, indicating that lower speeds combined with higher motor frequencies generate greater peak pressures. This behaviour may be attributed to the lower operating speed, which—when combined with a higher vibration frequency—allows the roller to remain in contact with the simulant for a longer duration per cycle, thereby imparting greater energy into the simulant.

Both Figures 6 and 7 illustrate that the roller-induced pressure is typically greatest near the ground surface and diminishes with depth, consistent with the findings of Rinehart & Mooney (2009) and Agarwal et al. (2025, under review). Figures 6 and 7 clearly demonstrate that an operating speed of 2 km/h at a motor frequency of 40 Hz produces the highest peak pressure at all measured depths compared with the other speed–frequency combinations with the roller mass of 2.92 kg. This observation aligns with the surface settlement measurements, which exhibited noticeable settlement at the roller speed of 2 km/h, further confirming the enhanced compaction efficiency achieved under these conditions.

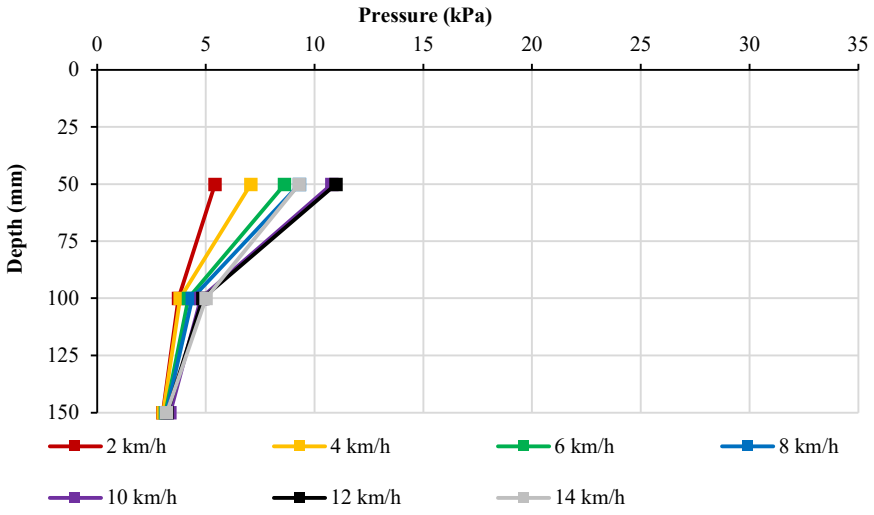

(a)

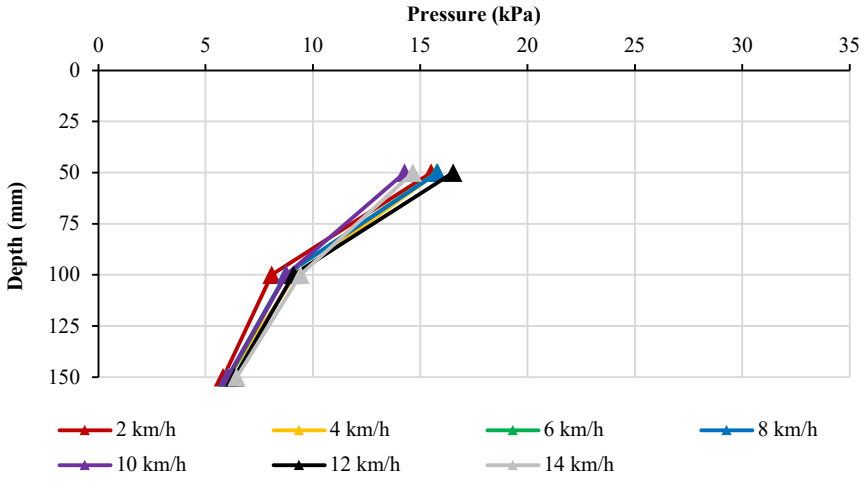

(b)

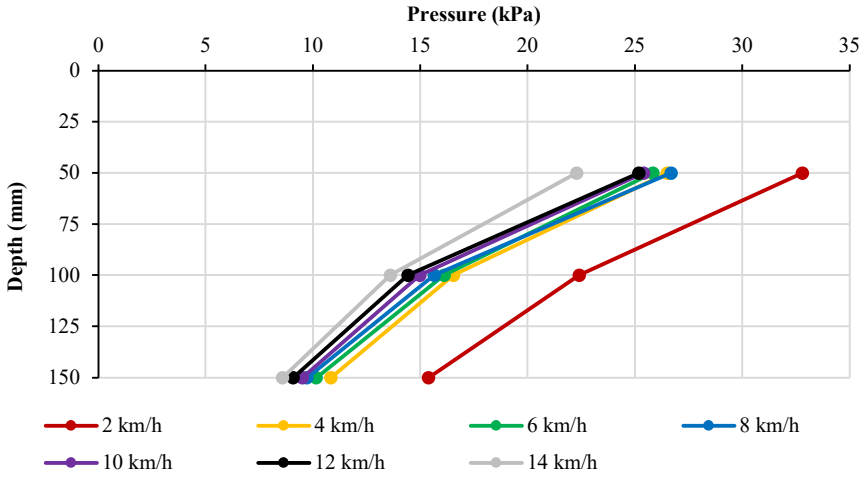

(c)

Figure 7. Peak pressure with depth for different operating speeds of LVDR-1 using a 2.92 kg drum roller, at fixed motor frequencies: (a) 20 Hz, (b) 30 Hz, and (c) 40 Hz.

A similar analysis conducted with the heavier drum roller mass of 4.45 kg exhibited the same behaviour as the 2.92 kg roller, with higher motor frequencies producing greater peak pressures at depth across all speeds tested. Figure 8. Peak pressure with depth for different operating speeds of LVDR-1 using a 4.45 kg drum roller, at 40 Hz motor frequencies. shows the measured peak pressures plotted against depth at a motor frequency of 40 Hz held constant, and the operating speed varied from 2 to 14 km/h, using a drum roller of 4.45 kg mass. From the data, an operating speed of 6 km/h at 40 Hz produced the highest peak pressures for the 4.45 kg mass across all combinations tested. When compared to 2.92 kg mass an operating speed of 2 km/h was found to be optimal. To better understand this discrepancy, a subsequent study is conducted below to compare the 2 km/h and 6 km/h operating speeds at constant frequency, roller mass and simulant density.

Across both roller masses, the findings confirm that motor frequency plays a dominant role in the compaction behaviour of the simulant. The results further indicate that increasing

the roller mass does not significantly enhance pressure response, a conclusion that aligns with the surface settlement measurements, which showed negligible variation with changes in roller mass after the 270th pass. Such insights are particularly valuable for optimising roller operation in lunar soil compaction applications, where effective transmission of compaction energy to deeper layers is critical.

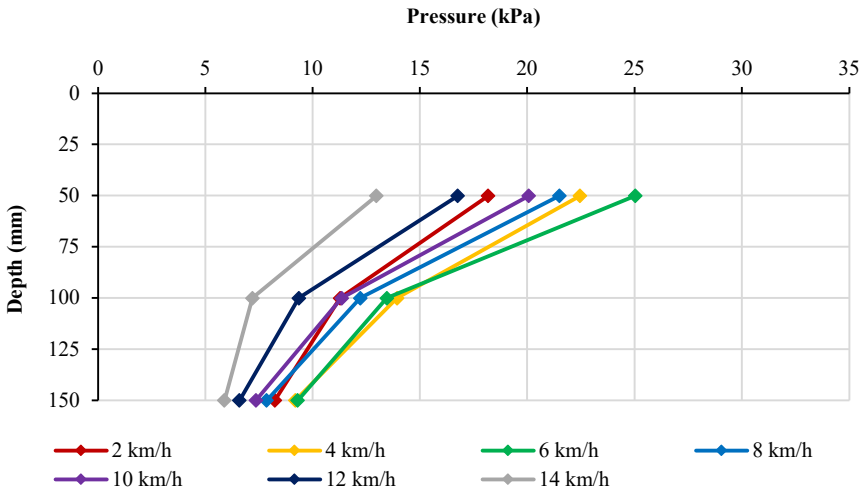

Figure 8. Peak pressure with depth for different operating speeds of LVDR-1 using a 4.45 kg drum roller, at 40 Hz motor frequencies.

Figure 9. Peak pressure with depth for two roller masses of LVDR-1 at 40 Hz across operating speeds of 2, 4, and 6 km/h. presents the peak pressures plotted against depth, illustrating the comparative performance of two roller masses under a constant vibration frequency of 40 Hz. Operating speeds of 2, 4, and 6 km/h are selected for both roller masses, as these conditions yielded the highest peak pressures across all tested speed–frequency combinations (refer to Figures 6, 7, and 8). Operating speeds above 6 km/h are not considered, as they did not yield effective compaction results, highlighting the importance of optimising roller speed in combination with vibration frequency to maximise energy transfer into the simulant. The results indicate that the maximum peak pressure of approximately 25 kPa was recorded at a depth of 50 mm for the 4.45 kg roller operating at 6 km/h, which is slightly lower than the 26 kPa measured for the 2.92 kg roller at 2 km/h. At a depth of 150 mm, the peak pressures were 9 kPa and 11 kPa for the 4.45 kg roller at 6 km/h and the 2.92 kg roller at 2 km/h, respectively, demonstrating that the lower-mass roller consistently produced higher pressures throughout the depth profile. This effect is particularly pronounced when compacting low-cohesion granular materials with a relatively high internal angle of friction, such as loosely packed lunar regolith simulant, where energy transfer and particle rearrangement are strongly influenced by the amplitude of vibration. (Look, 2022; Mooney & Rinehart, 2009). The 2.92 kg roller consistently exhibited higher peak pressures throughout the depth profile, suggesting that greater vibration amplitude facilitated more efficient energy transfer and particle rearrangement within the simulant. With increasing passes, the stiffness of the material increased, thereby reducing the magnitude of additional settlement per pass (Anderegg et al.,

2004). This change in surface stiffness in turn affects the vibration amplitude, influencing energy transmission and overall compaction performance.

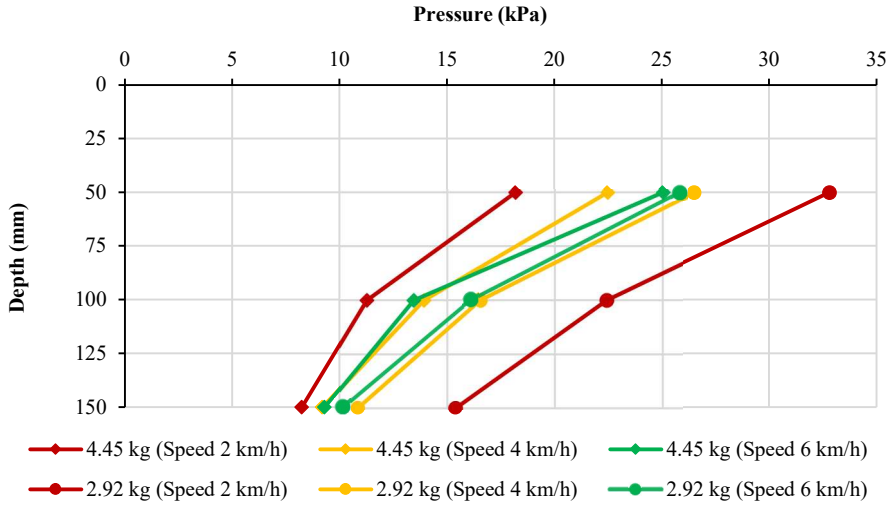

Figure 9. Peak pressure with depth for two roller masses of LVDR-1 at 40 Hz across operating speeds of 2, 4, and 6 km/h.

Figure 10. Vertical acceleration responses beneath the roller over a 1-second window at 50 mm depth and constant roller speed (6 km/h) and frequency (40 Hz) a) 2.92 kg and b) 4.45 kg. indicates that increasing the roller mass does not correlate with higher measured pressures. Figures 10(a) and 10(b) present the vertical acceleration response over a one-second window, spanning 0.5 seconds on either side of the time corresponding to the peak pressure. In Figure 10, the pressure cell depth (50 mm), roller speed (6 km/h), and motor frequency (40 Hz) were held constant, with only the roller mass varied.

It is evident from Figure 10(a) that the vertical (z-direction) acceleration amplitude is approximately three times greater than that observed in Figure 10(b). This indicates that the lighter roller mass generates a substantially larger dynamic response and therefore produces a greater in-ground acceleration response compared with the heavier roller mass.

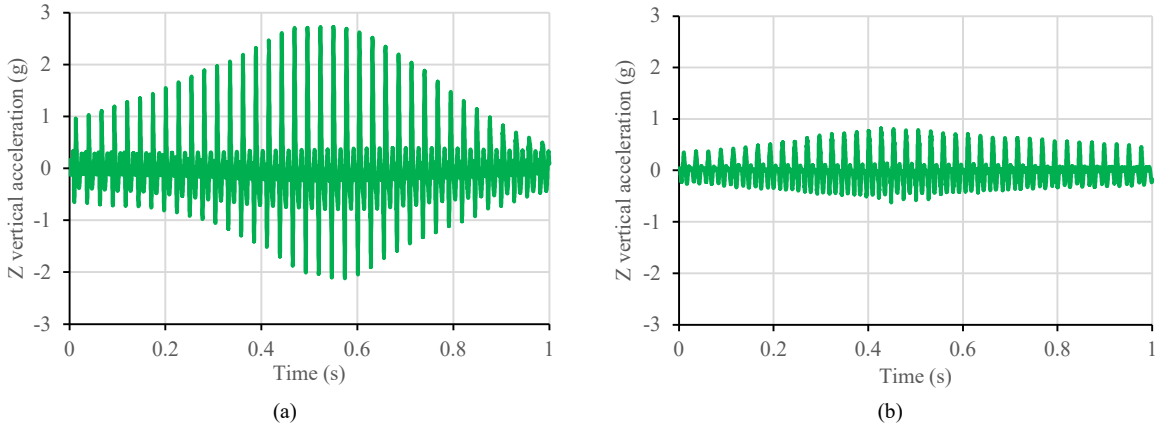

Figure 10. Vertical acceleration responses beneath the roller over a 1-second window at 50 mm depth and constant roller speed (6 km/h) and frequency (40 Hz) a) 2.92 kg and b) 4.45 kg.

To further examine the behaviour of the simulant within the influence zone beneath the roller, a 0.1-second window of the responses shown in Figures 10(a) and 10(b) are zoomed in and presented in Figures 11(a) and 11(b) for the 2.92 kg and 4.45 kg roller masses, respectively. Figures 11(a) and 11(b) illustrate the vertical acceleration time response, where an initial downward (negative) acceleration occurs as the simulant is loaded by the roller impacting the surface. Following this loading event, the resistance of the lunar simulant is mobilised, resulting in an upward acceleration. The acceleration-time response dampens and approaches zero, remaining near equilibrium until the next vibration cycle occurs approximately 0.025 seconds later, corresponding to the 40 Hz operating frequency of the roller. Future studies should therefore focus on measuring amplitude variations under different operating conditions to establish a clearer relationship between vibrational energy input, material stiffness changes and compaction performance.

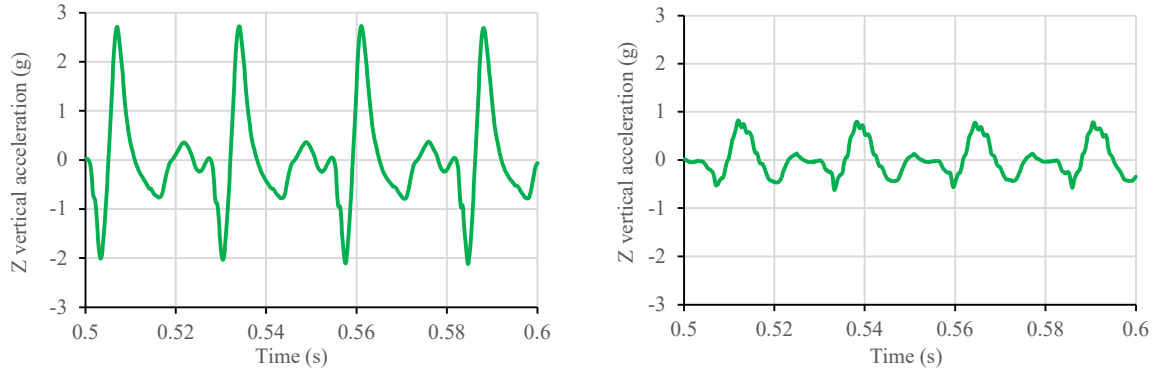

Figure 11. Vertical acceleration responses beneath the roller over a 0.1-second window at 50 mm depth and constant roller speed (6 km/h) and frequency (40 Hz) a) 2.92 kg and b) 4.45 kg.

5. CONCLUSION

This study presents the outcomes of an experimental investigation into the influence of operational parameters speed and motor frequency on the compaction performance of LHS-1E (engineering-grade lunar highland simulant) used as a terrestrial analogue for actual lunar highland regolith. The experiments were conducted using a scale vibrating smooth drum roller, incorporating two drum roller configurations with masses of 2.92 kg and 4.45 kg, respectively. The results demonstrate that both roller masses effectively densify the dry simulant, thereby affirming the feasibility of compacting lunar highland regolith simulant and highlighting the potential applicability of ground improvement techniques for lunar surface construction. The experimental investigation demonstrates that motor frequency has a more pronounced influence on simulant compaction than roller speed when using a vibrating smooth drum roller. Across all tests, a higher motor frequency of 40 Hz consistently produced the highest peak pressures at all measured depths, irrespective of operating speed and mass. The optimal combination of motor frequency and operating speed differs with roller mass: the lighter 2.92 kg mass achieved best results at 2 km/h and 40 Hz, whereas for the heavier 4.45 kg mass, 6 km/h and 40 Hz were found to be optimal. These findings emphasize that amplitude and

frequency of vibration are more influential than mass in achieving effective energy transfer to the regolith simulant and efficient subsurface compaction. While the method of increasing mass in this study is recognised as a simplification, future research will address this limitation through more advanced modelling and experimental approaches.

Overall, this study has tested key operational parameters, including speed, vibration and roller mass, thereby advancing the understanding of lunar highland regolith simulant behaviour. The results were consistent for drum roller masses of 2.92 kg and 4.45 kg, confirming that frequency is the dominant factor controlling dynamic soil response, while roller speed and mass play secondary roles. These findings highlight the importance of optimising motor frequency in lunar highland regolith compaction operations to achieve maximum peak pressure and effective depth penetration, providing valuable guidance for future lunar infrastructure construction and regolith stabilisation strategies. This knowledge is pivotal in informing the design of future in situ construction and surface operations on the Moon, where efficient material handling and compaction will be essential to mission success.

ACKNOWLEDGEMENTS

The authors would like to express their sincere gratitude to Kevin Farries, Dr. Yien Lik Kuo and Gary Bowman from Adelaide University for their invaluable support in the design and manufacture of the lunar vibrating drum roller (LVDR-1), as well as their assistance with laboratory testing. The authors also express their gratitude to the following final year, Civil Engineering Honours students from Adelaide University, who contributed to the testing outlined in this paper: Daniela Jaud, Nicolette Miller, Tasha Spratling and Lane Whittaker. The authors also extend their appreciation to Broons Impact Rollers for providing access to the test rig, which was essential for conducting the experimental work. Additionally, the authors acknowledge the facilities and technical support provided by the School of Civil Engineering and Construction Management at Adelaide University. This research was supported in part by institutional resources, and the contributions of all technical staff involved in the experimental setup and data acquisition are gratefully recognised.

REFERENCES

Agarwal, A.K., Jaksa, M.B.,Scott, B.T., Kuo, Y.L., 2025. Comparison of compaction techniques on lunar highland regolith simulant. Submitted to the ASCE Journal of Aerospace Engineering (under review).

Agarwal, A. K., Jaksa, M.B., Scott, B.T., Kuo, Y.L., 2024. Compaction testing on lunar highland simulant using a vibrating drum roller. In: *Earth and Space 2024: Engineering for Extreme Environments*, 19th ASCE Aerospace Division Biennial International Conference, Miami, FL, USA. https://doi.org/10.1061/9780784485736.068.

Agarwal, A.K., Kuo, Y.L., Jaksa, M.B., Scott, B.T., 2023. Density, strength and compressibility characteristics of lunar regolith simulant. *engrXiv*. https://doi.org/10.31224/6408 (Paper accepted for the 14th Australia and New

Zealand Conference on Geomechanics, Australian Geomechanics Society, Cairns, QLD, Australia).

Altaee, A., Fellenius, B.H., 1994. Physical Modeling in Sand. *Can. Geotech. J.* 31, 420 –431. https://doi.org/10.1139/t94-049.

Anderegg, R., Kaufmann, K., 2004. Intelligent compaction with vibratory rollers: Feedback control systems in automatic compaction and compaction control. *Transp. Res. Rec.* 1868(1), 124 –134. https://doi.org/10.3141/1868-13.

Carrier III, W.D., Olhoeft, G.R., Mendell, W., 1991. Physical properties of the lunar surface. In: Heiken, G., Vaniman, D.T., French, B.M. (Eds.), *Lunar sourcebook: A User's Guide to the Moon*, Cambridge University Press, Cambridge, pp. 475 –594.

Caterpillar Australia, 2025. Vibratory soil compactors. https://www.cat.com/en_AU/products/new/equipment/compactors/vibratory-soil-compactors.html (accessed 11 November 2025).

Chung, O.Y., Scott, B.T., Jaksa, M.B., Kuo, Y.L., Airey, D., 2017. Physical modelling of rolling dynamic compaction. In: *19th International Conference on Soil Mechanics in Geotechnical Engineering*, International Society for Soil Mechanics and Geotechnical Engineering (ICSMGE), Seoul, Korea, pp. 905–908.

Dave, T.N., Dasaka, S.M., 2011. A review on pressure measurement using earth pressure cell. *Int. J. Earth Sci Eng.* 4(6), 1031–1034.

Henrich, H., 1987. Compaction with vibratory rollers. *Civ. Eng. South Afr.* 1987(12), 479–481. https://journals.co.za/doi/pdf/10.10520/AJA10212019_16797.

Look, B.G., 2022. *Earthworks: Theory to Practice-Design and Construction*. CRC Press, London. https://doi.org/10.1201/9781003215486.

Mooney, M.A., Rinehart, R.V., 2009. In situ soil response to vibratory loading and its relationship to roller-measured soil stiffness. *J. Geotech. Geoenviron. Eng.* 135(8), 1022–1031. https://doi.org/10.1061/(ASCE)GT.1943-5606.0000046.

Oravec, H.A., 2009. *Understanding mechanical behavior of lunar soils for the study of vehicle mobility.* PhD dissertation, Case Western Reserve University, Cleveland, OH, USA.

Patrascu, D., 2022. Astrolab FLEX rover is here to help us build a life on extraterrestrial worlds. https://www.autoevolution.com/news/astrolab-flex-rover-is-here-to-help-us-build-a-life-on-extraterrestrial-worlds-199295.html (accessed 2 June 2025).

Rinehart, R.V. & Mooney M.A. 2009. Measurement of roller compactor induced triaxial soil stresses and strains. *Geotech. Test. J.* 32(4), 347–357. https://doi.org/10.1520/GTJ101889.

Space Resources Technologies, 2021. *Exolith lab LHS-1E Lunar Highlands Simulant: Fact Sheet 001-09-001-0120.* https://cdn.shopify.com/s/files/1/0398/9268/0862/files/lhs-1E-spec-sheet-2021.pptx_1.pdf?v=1693316297 (accessed 11 November 2025).

Scott, B., Jaksa, M. & Mitchell, P. 2019. Ground response to rolling dynamic compaction. *Geotech. Lett.* 9(2), 99–105. https://doi.org/10.1680/jgele.18.00208.

Scott, B.T., Kuo, Y.L., Jaksa, M.B. & Agarwal, A.K. 2023. Compaction trial on lunar regolith simulant. *engrXiv*. https://doi.org/10.31224/6410 (Paper accepted for the 14th Australia and New Zealand Conference on Geomechanics, Australian Geomechanics Society, Cairns, QLD, Australia).

Toklu, Y.C., Akpinar, P., 2022. Lunar soils, simulants and lunar construction materials: An overview. *Adv. Space Res.* 70(3), 762–779. https://doi.org/10.1016/j.asr.2022.05.017.

Vaniman, D., Reedy, R., Heiken, G., Olhoeft, G., Mendell, W. 1991. The lunar environment. In: Heiken, G.H., Vaniman, D.T., French, B.M. (Eds.), *Lunar Sourcebook: A User's Guide to the Moon*. Cambridge University Press, Cambridge, pp. 27–60.

Wersäll, C., 2016. *Frequency optimization of vibratory rollers and plates for compaction of granular soil*. PhD dissertation, KTH Royal Institute of Technology, Stockholm, Sweden.